

Bounds for shear viscosity in Nabarro-Herring-Coble creep

Laurence Brassart^{a,*}, Francis Delannay^b

^a*Department of Materials Science and Engineering,
Monash University, Clayton, VIC 3800, Australia*

^b*Institute of Mechanics, Materials and Civil Engineering (iMMC/IMAP),
Université catholique de Louvain, B-1348 Louvain-la-Neuve, Belgium*

Abstract

At high homologous temperature, plastic flow of a polycrystalline material can be mediated by self-diffusion and grain boundary sliding, rather than by dislocation glide. The effective viscosity of the polycrystal depends on the underlying mechanisms as well as on the microstructure. Simple expressions relating the shear viscosity to lattice and grain boundary diffusion coefficients were proposed in pioneering contributions by Nabarro and Herring [Herring, C., 1950. *J. Appl. Phys.* 21, 437-445] and Coble [Coble, R., 1963. *J. Appl. Phys.* 34, 1679-1682]. While these models remain widely used today to deduce the dominant mechanism based on the observed dependence of viscosity on grain size, a number of questions remain open. The present work revisits Nabarro-Herring-Coble creep using a micromechanical approach and variational principles. We focus on a random polycrystal of equiaxed grains deforming by coupled lattice and grain boundary diffusion and grain boundary sliding. We show that the classical results of Herring and Coble correspond to upper bounds on the shear viscosity, and obtain complementary lower bounds. Our results shed new light on these classical results and question the validity of the common interpretation of the dependence of viscosity on grain size.

Keywords: Diffusional creep, Grain boundary sliding, Effective behaviour, Variational principles

1. Introduction

Nabarro (Nabarro, 1948) and Herring (Herring, 1950) were the first to propose that, under low stress, creep of a polycrystalline solid can proceed without dislocation activity by diffusional flow from grain boundaries under normal compression toward grain boundaries under normal tension. Owing to the linear dependence of the diffusion potential on the stress normal to a grain boundary (Herring, 1950; Green, 1970; Herring, 1971; Balluffi et al., 2005), such a deformation mechanism should bring about a linearly viscous macroscopic behaviour. According to Herring's model (Herring, 1950), if diffusion occurs only through the bulk of the lattice, the macroscopic viscosity is proportional to the square of grain size. Noticing that diffusion at low homologous temperature may be restricted to a thin layer close to grain boundaries, Coble (Coble, 1963) complemented Herring's model by showing that viscosity should then vary as the third power of grain size. The Nabarro-Herring-Coble (NHC) creep model has been very widely adopted in the materials community and the pioneering papers of Nabarro, Herring and Coble remain today very

*Corresponding author. Email: laurence.brassart@monash.edu

commonly cited in the literature, in particular in relation to the grain-size dependence of creep rate and sintering rate.

Based on these papers, many authors have worked out models for establishing the link between the macroscopic creep rate and the mechanisms underlying NHC creep (Gibbs, 1966; Green, 1970; Raj and Ashby, 1971; Beere, 1976, 1977, 1978; Spingarn and Nix, 1978; Greenwood, 1985, 1992; Pan and Cocks, 1993; Burton, 1994; Cocks, 1996; Mori et al., 1997; Koblinski et al., 1998; Mori et al., 1998a; Onaka et al., 1998; Mori et al., 1998b; Onaka et al., 2001; Kim et al., 2003, 2004; Wei et al., 2008; Wang et al., 2011; Hötzer et al., 2019). The objective of the present paper is to shed a new light on the dependence of NHC creep rate on material parameters via the use of variational principles, which define upper and lower bounds for the macroscopic viscosity, G , of a polycrystal (Needleman and Rice, 1980; Cocks, 1994). Although reference to such bounds has already been made in connection with modelling of diffusional deformation (Ashby et al., 1978; McMeeking and Kuhn, 1992; Cocks, 1996), what these bounds imply for NHC creep has not been thoroughly analysed yet. It will be shown that the NHC model actually corresponds to an upper bound for G , and that complementary lower bounds can also be obtained. The results will question in particular the validity of the classical interpretation of the dependence of viscosity on grain size.

The basics of the NHC creep mechanism are that a velocity difference between adjacent grains in direction normal to grain boundary can arise via the emission or absorption of vacancies at grain boundaries, where all sources and sinks of vacancies are supposed to be localised. At the microscopic scale, the mechanism can be apprehended in terms of climb of grain boundary dislocations (GBDs) (Gleiter et al., 1968) having a Burgers vector perpendicular to the boundary. The rate-governing parameters of dislocation climb are the vacancy diffusivities, in the bulk of the lattice and in a layer of thickness δ along the grain boundary. Ashby and co-workers have discussed in terms of GBDs the imperfect character of the grain boundary as source and sink of vacancies, which brings about departure from purely Newtonian viscous behaviour (Ashby, 1969, 1972; Arzt et al., 1983).

However, Lifshitz (Lifshitz, 1963) was the first to emphasize the fact that it is not possible to account for the component of velocity difference parallel to grain boundary if emission/absorption of vacancies is not accompanied by sliding along grain boundaries. He proposed to represent the resistance to grain boundary sliding by a linear law:

$$\sigma_t = \eta \Delta v_t, \quad (1)$$

where σ_t is the shear stress tangent to grain boundary, Δv_t is the tangent component of the grain velocity difference, and η is a friction coefficient. It follows that macroscopic viscosity involves, in addition to the dissipation considered by Herring and Coble, a contribution due to resistance to grain boundary sliding. If η is large, dissipation could become dominated by the latter contribution and viscosity would then tend to vary linearly with grain size.

At the microscopic scale, the mechanism of grain-boundary sliding can be apprehended in terms of glide of GBDs having Burgers vector parallel to the boundary (Ashby, 1972; Crossman and Ashby, 1975; Bilde-Sørensen and Smith, 1994). The friction coefficient η should then be linked to the critical resolved shear stress for GBD glide, which is largely unknown and not accessible experimentally. In early models, authors circumvented this difficulty by advocating that dissipation due to grain boundary friction should be negligible with respect to dissipation due to diffusion because GBD glide amounts to the displacement of a collection of atoms at the scale of lattice parameter whereas GBD climb

requires vacancy diffusion at grain scale (Gibbs, 1968; Burton, 2002). However, as noticed by Beere (Beere, 1977, 1978), periodic arrays of parallelepipeds deforming according to the NHC mechanism would collapse like a pack of cards if boundary friction stresses were null. Analyses taking full account of the coupling of diffusion and frictional sliding at grain boundaries were proposed by Mori and co-workers (Mori et al., 1998a,b; Onaka et al., 1998, 2001) and by Kim and co-workers (Kim et al., 2004, 2005a,b, 2009).

Beside the role of boundary friction forces, question marks also aroused from experimental observations revealing that the magnitude of (i) grain boundary sliding measured by line tracing methods (Gifkins and Langdon, 1970) and (ii) grain elongation measured after superplastic forming are, respectively, larger and smaller than what should correspond to the NHC mechanism. This issue led Cannon (Cannon, 1972) to introduce the distinction between two types of grain boundary sliding: "Lifshitz sliding", which is the sliding required for the respect of compatibility conditions between adjacent grains during the NHC deformation mode, and "Rachinger sliding", which brings about a different deformation mode involving grain rearrangement by relative motion of grains that remain equiaxed (Rachinger, 1952-1953). Like most former models in literature, the present paper considers only Lifshitz sliding. Extension of the approach to Rachinger sliding will be the subject of another paper.

After introducing in Section 2 the governing equations describing local and effective flow behaviours of polycrystals, we present in Section 3 the basics of the variational formulation of the problem, which brings to the concepts of kinematic/upper bounds and statical/lower bounds for the shear viscosity. In Section 4, these concepts are applied to the modelling of deformation of a randomly isotropic polycrystal in conditions of co-existence of lattice diffusion and grain boundary diffusion. Like in Herring's model, the representative unit cell is taken to be a spherical grain. Variational principles yield expressions for the dependence of upper and lower bounds of G on grain size, lattice and grain boundary diffusion coefficients D_l and D_b , and friction coefficient η . Whereas the upper bound expression largely agrees with former models in the literature, the expression for the corresponding lower bound has not been reported previously. The results are discussed in Section 5, which focuses in particular on the dependence of the grain size sensitivity exponent on η .

2. Governing equations

2.1. Local behaviour

We consider a dense aggregate of rigid grains deforming by a combination of diffusional creep and grain boundary sliding (Fig. 1a). Diffusion in the bulk of the grains is mediated by a vacancy-exchange mechanism, and we neglect the creation and annihilation of vacancies within the bulk. The driving force for atomic diffusion is the gradient of the difference between the chemical potential of the atoms, μ_A and that of the vacancies, μ_V . Introducing the diffusion potential $\mu = \mu_A - \mu_V$, we express the lattice (volumetric) diffusion flux (in units of length/time) as (Herring, 1950):

$$\mathbf{j}_l = -\frac{D_l}{kT} \nabla \mu, \quad (2)$$

where k is Boltzmann's constant and T is the absolute temperature. The lattice diffusion coefficient D_l (in units of $\text{length}^2/\text{time}$) is related to the vacancy diffusion coefficient D_V by $D_l = D_V X_V$, where X_V is the atom fraction of vacancies (Balluffi et al., 2005). We

assume that variations of X_V throughout the crystal are small, and treat the diffusion coefficient D_l as a constant. Assuming that diffusion is in quasi steady-state, the equation of conservation of atoms writes:

$$\nabla \cdot \mathbf{j}_l = 0. \quad (3)$$

It follows from Eqs (2) and (3) that $\nabla^2 \mu = 0$ in the bulk of a grain. The diffusion potential on the boundary is related to the normal stress σ_n by (Herring, 1950, 1971):

$$\mu = \mu_A^\circ - \Omega \sigma_n - \mu_V = \mu_A^\circ - \Omega \sigma_n, \quad (4)$$

where μ_A° is a reference chemical potential (usually taken as the free energy per atom in an infinitely-extended, vacancy-free crystal) and Ω is an average volume per atom. In the rest of the paper, we will set $\mu_A^\circ = 0$, without loss of generality. Expression (4) describes the reduction in potential energy of the system due to the insertion of an atom below the boundary under traction. The second equality in Eq. (4) follows from the assumption that grain boundaries act as ideal sources and sinks for vacancies, so that the vacancies are maintained at their equilibrium concentration near the interface and $\mu_V = 0$ (Balluffi et al., 2005).

The grain boundary is considered to consist of a thin layer of thickness δ in which the diffusion coefficient D_b (in units of length²/time), is different from the lattice diffusion coefficient D_l . The volumetric diffusion flux inside the grain boundary (in units of length/time) is given by:

$$\mathbf{j}_b = -\frac{\delta D_b}{kT} \nabla_s \mu, \quad (5)$$

where ∇_s denotes the gradient operator on the grain boundary surface and μ is given by Eq. (4). Conservation of matter at grain boundary junctions requires that:

$$\sum \mathbf{j}_b \cdot \mathbf{m} = 0, \quad (6)$$

where the summation extends over the grain boundaries meeting at a junction and \mathbf{m} is the outward normal to the arc of intersection within the grain boundary plane of each participating grain facet.

The difference of velocity, Δv_n between adjacent grains in the direction normal to the grain boundary is supposed to have only two possible origins: the normal component of \mathbf{j}_l on the surface of each grain, and the divergence of \mathbf{j}_b in the grain boundary surface:

$$\Delta v_n = -(\mathbf{j}_l^{(+)} - \mathbf{j}_l^{(-)}) \cdot \mathbf{n} - \nabla_s \cdot \mathbf{j}_b, \quad (7)$$

where the superscripts $(-)$ and $(+)$ refer to the two adjacent grains and \mathbf{n} is the outward normal to grain $(-)$ pointing towards grain $(+)$, see Fig. 1b. The tangential difference of velocity, Δv_t between adjacent grains is supposed to be linearly related to the tangential stress on the grain boundary surface:

$$\Delta v_t = \frac{1}{\eta} \sigma_t, \quad (8)$$

where σ_t is the shear stress on the surface and η is a friction coefficient characterizing the sliding mechanism operating at microscopic scale.

The field of stress must satisfy mechanical equilibrium in grain interior, $\nabla \cdot \boldsymbol{\sigma} = \mathbf{0}$, and tractions must equilibrate at grain boundaries: $(\boldsymbol{\sigma}^{(-)} - \boldsymbol{\sigma}^{(+)}) \cdot \mathbf{n} = \mathbf{0}$. We also assume that the internal grain-boundary tensions are at equilibrium. Mechanical boundary conditions can be written in terms of prescribed velocity or prescribed traction components on the external surface of the aggregate. Chemical boundary conditions can be specified in terms of prescribed net flux or prescribed diffusion potential on the external surface.

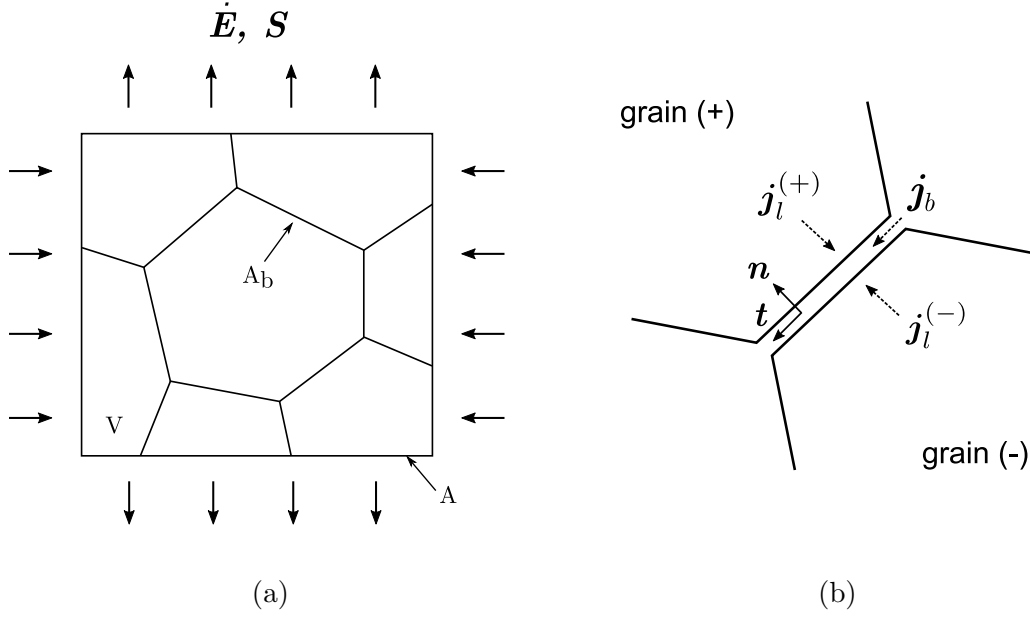


Figure 1: (a) An aggregate of grains subject to a macroscopic strain rate $\dot{\mathbf{E}}$ or a macroscopic stress \mathbf{S} via prescribed velocity or prescribed traction boundary conditions applied to the external surface A . The aggregate contains grains with total volume V meeting at grain boundaries with total surface A_b . (b) Deformation of the aggregate is mediated by surface diffusion along the grain boundaries, lattice diffusion within the grains and sliding along grain boundaries.

2.2. Effective behaviour

The effective behaviour of the aggregate is described by the relationship between the average (macroscopic) strain rate $\dot{\mathbf{E}}$ and the average stress \mathbf{S} in a Representative Volume Element (RVE) of the aggregate. We focus on steady-state creep, i.e. we assume that all transient contributions to stress and diffusion fields during initial elastic loading of the polycrystal have relaxed. Relaxation kinetics towards steady-state was previously investigated in 2D by Mori et al. (1998a) and Onaka et al. (1998). Accounting for the velocity discontinuity at the grain boundaries, the macroscopic strain rate is defined as:

$$\dot{E}_{ij} = \frac{1}{2V} \int_A (v_i n_j + v_j n_i) dA \quad (9)$$

$$= \frac{1}{2V} \int_{A_b} (\Delta v_i n_j + \Delta v_j n_i) dA \quad (10)$$

where V is the total volume of the aggregate, A denotes the external surface of the aggregate and A_b denotes the grain boundary area, see Fig. 1a. In the case of deformable grains and when the velocity field is continuous, the first equality is equivalent to the usual definition of macroscopic strain rate as the volume average of the microscopic strain rate. The second equality is obtained using the divergence theorem and accounting for the rigidity of the grains.

The macroscopic stress is defined as:

$$S_{ij} = \frac{1}{2V} \int_A (T_i x_j + T_j x_i) dA \quad (11)$$

$$= \frac{1}{V} \int_V \sigma_{ij} dV \quad (12)$$

where x_i is the position vector and $T_i = \sigma_{ij}n_j$ the traction vector on the external surface of the aggregate. The second equality follows from the equilibrium of tractions across grain boundaries and the condition of mechanical equilibrium in the grain interior.

In a classical micromechanics approach, the effective behaviour of the aggregate is obtained as follows. In the case where the macroscopic strain rate $\dot{\mathbf{E}}$ is prescribed, velocity boundary conditions are chosen such that equality (9) is satisfied. After solving the boundary-value problem, the macroscopic stress \mathbf{S} is calculated using Eq. (12). Alternatively, in the case where the macroscopic stress \mathbf{S} is prescribed, traction boundary conditions are chosen such that equality (11) is satisfied. After solving the boundary-value problem, the macroscopic strain rate $\dot{\mathbf{E}}$ is calculated using Eq. (10). We assume that Hill's condition holds (Hill, 1967):

$$V\mathbf{S} : \dot{\mathbf{E}} = \int_A \mathbf{T} \cdot \mathbf{v} dS, \quad (13)$$

which states the equality of the macroscopic and average microscopic powers expended in the RVE. This condition is satisfied by affine velocity boundary conditions for a prescribed strain rate, $\mathbf{v} = \dot{\mathbf{E}} \cdot \mathbf{x}$ on A , and by uniform traction boundary conditions for a prescribed macroscopic stress, $\mathbf{T} = \mathbf{S} \cdot \mathbf{n}$ on A .

We verify that the effective behaviour resulting from the local equations summarised in Section 2 is incompressible. According to Eq. (10), the volumetric strain rate is related to the normal velocity discontinuity at grain boundaries by:

$$V\dot{E}_{kk} = \int_{A_b} \Delta v_n dA. \quad (14)$$

Using the continuity equation (7) and the divergence theorem, we obtain:

$$V\dot{E}_{kk} = \int_{\Gamma_b} - \sum (\mathbf{j}_b \cdot \mathbf{m}) dL + \int_V \nabla \cdot \mathbf{j}_l dV \quad (15)$$

$$= 0. \quad (16)$$

In writing Eq. (15), we have implicitly assumed zero-net lattice and boundary flux boundary conditions. The first term on the right-hand side vanishes according to Eq. (6) and the second term vanishes according to Eq. (3). Incompressibility implies that, for prescribed strain rate, the macroscopic stress can only be calculated up to an undetermined hydrostatic stress. If the aggregate is isotropic, the effective behaviour is fully characterised by the macroscopic shear viscosity G , defined as:

$$G = \frac{S'_{ij}}{2\dot{E}'_{ij}} = \frac{S'_{ij}}{2\dot{E}_{ij}}, \quad (17)$$

where the notation $(\cdot)'$ refers to the deviatoric part of a second-order tensor. The macroscopic bulk viscosity K is infinite.

3. Variational principles

The governing equations presented in the previous section can be recast in variational form. The kinematic variational principle given below was first derived by Needleman and Rice (1980) for coupled grain-boundary diffusion and dislocation-mediated plasticity. Several variations were subsequently proposed to also describe grain-boundary sliding (McMeeking and Kuhn, 1992), interface reaction (Cocks, 1994) and lattice diffusion

(Cocks, 1996). Complementary statical variational principles were derived by Cocks (1994, 1996). The variational principles form the basis of Galerkin-type finite-element procedures for simulating the evolution of material surfaces at microscopic scale, see for example (Pan and Cocks, 1993; Suo, 1997; Cocks et al., 1998) or more recently (Wei et al., 2008). Here, we use variational principles in order to obtain bounds on the effective shear viscosity.

3.1. Kinematic variational principle

Consider an aggregate subject to prescribed velocity boundary conditions on the portion A_V of its external surface, and to prescribed traction boundary conditions on the portion A_T of its external surface, such that $A_V \cup A_T = A$ and $A_V \cap A_T = \emptyset$. The kinematic variational principle states that, among all the kinematically admissible velocity fields and diffusion flux fields, the actual fields *minimise* the following functional:

$$I = \Psi - \frac{1}{V} \int_{A_T} \bar{\mathbf{T}} \cdot \mathbf{v} \, dA, \quad (18)$$

where Ψ is a dissipation potential given by:

$$\Psi = \frac{1}{V} \left[\int_V \frac{1}{2} \frac{kT}{\Omega D_l} \mathbf{j}_l \cdot \mathbf{j}_l \, dV + \int_{A_b} \left(\frac{1}{2} \frac{kT}{\Omega \delta D_b} \mathbf{j}_b \cdot \mathbf{j}_b + \frac{1}{2} \eta (\Delta v_t)^2 \right) dA \right]. \quad (19)$$

The second term of Eq. (18) represents the potential energy of the applied tractions, with $\bar{\mathbf{T}}$ the prescribed traction vector on A_T . An admissible velocity field is such that its gradient vanishes in the grain interior (rigid grains), and such that the normal velocity jump across grain boundaries is related to the diffusion flux fields by the continuity condition (7). The velocity field should also comply with the prescribed velocity on A_V . An admissible lattice diffusion flux field is divergence-free in the grain interior; an admissible grain boundary flux field is such that condition (6) is satisfied at the grain boundary junctions. The proof that the functional (18) is stationary for the exact fields can be found in (McMeeking and Kuhn, 1992) and (Cocks, 1996), and elements of the proof are provided in Appendix A.1.

The kinematic minimum principle is analogous to the Potential Energy Theorem for elastic solids (Duvaut, 1990; Doghri, 2000). In the context of thermodynamic extremal principles (Fischer et al., 2014), the kinematic variational principle corresponds to the Minimum Principle for the the Dissipation Potential”, and we refer to (Fischer et al., 2014; Hackl and Fischer, 2008) for a comparison of this principle to other thermodynamic extremal principles.

We consider the situation where the macroscopic strain rate $\dot{\mathbf{E}}$ is prescribed via velocity boundary conditions on the external surface of the aggregate. In this case $A = A_V$ and $A_T = \emptyset$, and thus $I = \Psi$. Evaluation of the dissipation potential for the exact fields together with Hill’s condition (13) leads to the equality (see Eq. (72) in Appendix A.1):

$$\Psi = \frac{1}{2} \mathbf{S} : \dot{\mathbf{E}} = G \dot{\mathbf{E}} : \dot{\mathbf{E}}. \quad (20)$$

Let Ψ^c be the value of the dissipation potential calculated for admissible, not-necessarily exact fields. By analogy with Eq. (20), we define the corresponding estimate of the shear viscosity, G^+ , as:

$$\Psi^c = G^+ \dot{\mathbf{E}} : \dot{\mathbf{E}}. \quad (21)$$

According to the minimum principle, $\Psi \leq \Psi^c$, and therefore G^+ constitutes an *upper bound* on the shear viscosity: $G^+ \geq G$.

3.2. Statical variational principle

Consider again an aggregate subject to prescribed velocity boundary conditions on the portion A_V of its external surface, and to prescribed traction boundary conditions on the portion A_T of its external surface. The complementary statical variational principle states that, among all admissible fields of stress and diffusion potential, the actual ones *minimise* the functional:

$$J = \Phi - \frac{1}{V} \int_{A_V} \mathbf{T} \cdot \bar{\mathbf{v}} \, dA, \quad (22)$$

where the dual dissipation potential Φ is given by:

$$\Phi = \frac{1}{V} \left[\int_V \frac{1}{2} \frac{D_l}{\Omega k T} \nabla \mu \cdot \nabla \mu \, dV + \int_{A_b} \left(\frac{1}{2} \frac{\delta D_b}{\Omega k T} \nabla_s \mu \cdot \nabla_s \mu + \frac{1}{2\eta} \sigma_t^2 \right) dA \right]. \quad (23)$$

In the second term of Eq. (22), $\bar{\mathbf{v}}$ represents the prescribed velocity on A_V . An admissible stress field satisfies the conditions of mechanical equilibrium in the grain interior and across grain boundaries. It also satisfies the traction boundary conditions on A_T . An admissible field of diffusion potential is such that $\mu = -\Omega \sigma_n$ on the grain boundary. The proof that the functional (22) is minimised for the exact fields is outlined in Appendix A.1. The statical variational principle is analogous to the Principle of Maximum Complementary Energy in elasticity (Doghri, 2000).

In the case where the macroscopic stress \mathbf{S} is prescribed via traction boundary conditions on the external surface, $A_T = A$, $A_V = \emptyset$, and therefore $J = \Phi$. Evaluating the dual dissipation potential for the exact fields and using Hill's condition (13) leads to (see Eq. (74) of Appendix A.1):

$$\Phi = \frac{1}{2} \mathbf{S}' : \dot{\mathbf{E}} = \frac{\mathbf{S}' : \mathbf{S}'}{4G}. \quad (24)$$

Let Φ^* be the value of the dual dissipation potential calculated for admissible, not-necessarily exact fields. By analogy with Eq. (24), the corresponding estimate G^- of the shear modulus is defined as:

$$\Phi^* = \frac{\mathbf{S}' : \mathbf{S}'}{4G^-}. \quad (25)$$

Since $\Phi \leq \Phi^*$, it follows that the shear viscosity G^- calculated from Φ^* constitutes a *lower bound* on the actual shear viscosity G : $G^- \leq G$.

In Appendix A.2, it is shown that the exact shear modulus of an aggregate subject to affine velocity boundary conditions is larger or equal to the exact shear modulus of the same aggregate subject to uniform traction boundary conditions. This result is analogous to the corresponding result for the elastic modulus of random aggregates, see e.g. Huet (1990). As the number of grains in the random aggregate increases, the discrepancy between the moduli obtained with the two types of boundary conditions decreases as the effective behaviour becomes less sensitive of the detail of the applied boundary conditions. By definition, the effective behaviour of a true RVE of the microstructure should be independent of the type of boundary conditions.

4. Model for isotropic polycrystal

We consider a randomly isotropic polycrystal with equiaxed grains and we assume that grain boundaries are randomly distributed and on average oriented perpendicular to the line joining the centres of gravity of two adjacent grains. Consequently, we consider

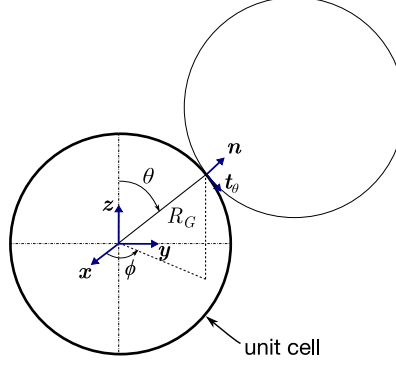


Figure 2: Unit cell containing one representative spherical grain. Grain boundaries are randomly distributed on the unit cell surface and oriented perpendicular to the line joining the centres of two adjacent cells.

as representative unit cell a spherical grain with radius R_G and volume equal to the average grain volume which is in contact with an identical spherical grain at each point of its surface (McMeeking and Kuhn, 1992). The spherical grain model is convenient to illustrate the variational principles because it is amenable to simple analytical treatment. It also allows us to establish connections with classical results for Nabarro-Herring and Coble creep (Herring, 1950; Coble, 1963), which also relied on the spherical grain geometry, as well as more recent results by Onaka et al. (2001) who also accounted for non-zero friction coefficient. We will show that these classical results can be recovered as special case using the kinematic variational principle. In addition, new lower bounds based on the statical variational principle will be derived.

The spherical unit cell is represented in Fig. 2. The Cartesian components of the unit vector \mathbf{n} normal to the representative sphere write

$$\mathbf{n} = \begin{pmatrix} \sin \theta \cos \phi \\ \sin \theta \sin \phi \\ \cos \theta \end{pmatrix}, \quad (26)$$

whereas the components of a unit vector \mathbf{t}_θ and \mathbf{t}_ϕ tangent to the grain boundary in the longitudinal and azimuthal directions write

$$\mathbf{t}_\theta = \begin{pmatrix} \cos \theta \cos \phi \\ \cos \theta \sin \phi \\ -\sin \theta \end{pmatrix}, \quad \mathbf{t}_\phi = \begin{pmatrix} -\sin \phi \\ \cos \phi \\ 0 \end{pmatrix}. \quad (27)$$

4.1. Kinematic bound

We first consider the case where the macroscopic strain rate is prescribed, and aim at estimating the corresponding macroscopic shear viscosity using the kinematic variational principle (Section 3.1). The macroscopic strain rate is chosen of the following form:

$$\dot{\mathbf{E}} = \begin{pmatrix} -\frac{\dot{E}}{2} & 0 & 0 \\ 0 & -\frac{\dot{E}}{2} & 0 \\ 0 & 0 & \dot{E} \end{pmatrix}. \quad (28)$$

Then, according to Eqs (19) and (21), an upper bound for the shear viscosity is obtained as:

$$G^+ = \frac{2\Psi}{3\dot{E}^2}, \quad (29)$$

where Ψ is expressed as:

$$\begin{aligned} \Psi &= \Psi_l + \Psi_b + \Psi_{sl} \\ &= \frac{1}{V_G} \int_{V_G} \frac{kT}{2\Omega D_l} \mathbf{j}_l \cdot \mathbf{j}_l dV + \frac{1}{2V_G} \int_{A_G} \frac{kT}{2\Omega \delta D_b} \mathbf{j}_b \cdot \mathbf{j}_b dA \\ &\quad + \frac{1}{2V_G} \int_{A_G} \frac{1}{2} \eta (\Delta v_t)^2 dA, \end{aligned} \quad (30)$$

which should be calculated for a set of admissible velocity and diffusion fields compatible with the macroscopic strain rate. Compared to the general expression (19), the additional (1/2) pre-factor in front of the the surface integrals accounts for the fact that contact points on the unit cell surface are shared between two grains.

A simple trial velocity field is obtained by assuming that the relative motion of the centres of adjacent grains comply with the macroscopic strain rate (Fleck et al., 1992; McMeeking and Kuhn, 1992):

$$\Delta v_i = 2R_G \dot{E}_{ij} n_j. \quad (31)$$

This choice indeed satisfies equality (10), taking A_b as the area of the spherical unit cell and accounting for the fact that contacts points are shared between two grains. (Note that in the spherical grain model, external boundaries of the aggregate are not represented and Eq. (9) cannot be used.) The normal and tangential components of $\Delta \mathbf{v}$ are calculated as

$$\Delta v_n = \Delta \mathbf{v} \cdot \mathbf{n} = \frac{3}{2} R_G \dot{E} \left(\cos 2\theta + \frac{1}{3} \right) \quad (32)$$

and

$$\Delta v_t = \Delta \mathbf{v} \cdot \mathbf{t}_\theta = -\frac{3}{2} R_G \dot{E} \sin 2\theta. \quad (33)$$

Admissible diffusion fluxes in the lattice and on the grain boundary surface must be proposed in such a way that the continuity condition (7) is satisfied. For the spherical unit cell model, this condition particularises as:

$$\Delta v_n = 2j_{lr} - \nabla \cdot \mathbf{j}_b, \quad (34)$$

since two identical grains meet at each contact point on the unit cell surface. We consider a class of trial diffusion fluxes of the following form:

$$j_{lr}(r, \theta) = \frac{3}{4} \alpha r \dot{E} \left(\cos 2\theta + \frac{1}{3} \right) \quad (35)$$

$$j_{l\theta}(r, \theta) = -\frac{3}{4} \alpha r \dot{E} \sin 2\theta \quad (36)$$

$$j_{l\phi}(r, \theta) = 0 \quad (37)$$

and

$$j_{b\theta}(\theta) = \frac{1}{2} \beta R_G^2 \dot{E} \sin(2\theta), \quad j_{b\phi}(\theta) = 0 \quad (38)$$

where α and β are constant parameters. It can be verified that the trial lattice flux (35)-(37) is divergence-free and satisfies the symmetry condition $\mathbf{j}_l(0, \theta) = \mathbf{0}$. On the

other hand, the trial grain-boundary flux (38) satisfies the symmetry condition $\mathbf{j}_b(0) = \mathbf{j}_b(\pi/2) = \mathbf{0}$. These fluxes satisfy the continuity condition (34) provided that the parameters α and β are related by:

$$\alpha - \beta = 1. \quad (39)$$

Each pair (α, β) satisfying the above constraint thus leads to admissible diffusion flux fields compatible with the prescribed velocity discontinuity.

Inserting expressions (35)-(38) into expression (30), the diffusion contribution to the potential Ψ is calculated:

$$\Psi_d = \Psi_l + \Psi_b = \frac{1}{5} \frac{kTR_G^3}{\Omega\delta D_b} \dot{E}^2 \left(\frac{3}{4\Delta} \alpha^2 + \beta^2 \right), \quad (40)$$

where we introduced the notation $\Delta = D_l R_G / \delta D_b$. The diffusion contribution to the upper bound on the viscosity is in turn calculated from Eq. (29):

$$G_d^+ = \frac{2\Psi_d}{3\dot{E}^2} = \frac{1}{15} \frac{kTR_G^3}{\Omega\delta D_b} \left(\frac{3}{2\Delta} \alpha^2 + \beta^2 \right). \quad (41)$$

Grain boundary sliding bring an additional contribution to the potential (30), which, using Eq. (33) expresses as:

$$\Psi_{sl} = \frac{9}{10} \dot{E}^2 R_G \eta. \quad (42)$$

According to Eq. (29), the contribution of grain boundary sliding to the upper bound of viscosity is thus:

$$G_{sl}^+ = \frac{2\Psi_{sl}}{3\dot{E}^2} = \frac{3}{5} \eta R_G, \quad (43)$$

which is independent of the choice of parameters α and β .

The optimal (i.e. lowest) upper bound on the shear viscosity is obtained by finding the parameters α and β which minimise the potential (40) under the constraint (39). This is easily achieved using a Lagrange multiplier, and leads to:

$$\alpha = \left(1 + \frac{3}{2\Delta} \right)^{-1}, \quad \beta = -\frac{3\alpha}{2\Delta} = -\left(1 + \frac{2\Delta}{3} \right)^{-1}. \quad (44)$$

The diffusion contribution to the upper bound on the shear viscosity is illustrated in Fig. 3 as a function of parameter α , for different value of Δ . The optimal value of α (indicated by a circle on the figure) shifts from $\alpha = 0$ for $\Delta \rightarrow 0$ (grain boundary diffusion-dominated, $\beta = -1$) to $\alpha = 1$ for $\Delta \rightarrow \infty$ (lattice diffusion-dominated, $\beta = 0$).

Using the optimal choice of parameters (44) in Eq. (41) and adding the sliding contribution (43), the lowest upper bound on the shear viscosity is finally obtained:

$$G^+ = G_d^+ + G_{sl}^+ = \frac{1}{15} \left(1 + \frac{2\Delta}{3} \right)^{-1} \frac{kTR_G^3}{\Omega\delta D_b} + \frac{3}{5} \eta R_G. \quad (45)$$

When $\Delta \gg 1$, grain boundary diffusion is negligible relative to lattice diffusion, and the viscosity reduces to:

$$G_l^+ = \frac{kTR_G^2}{\Omega D_l} \left(\frac{1}{10} + \frac{3}{5} \eta_l \right), \quad (46)$$

with $\eta_l = \eta \left(\frac{\Omega D_l}{kTR_G} \right)$. The first term on the right-hand side of Eq. (46) (lattice diffusion contribution) is identical to the result of Onaka et al. (2001), who used the same kinematic

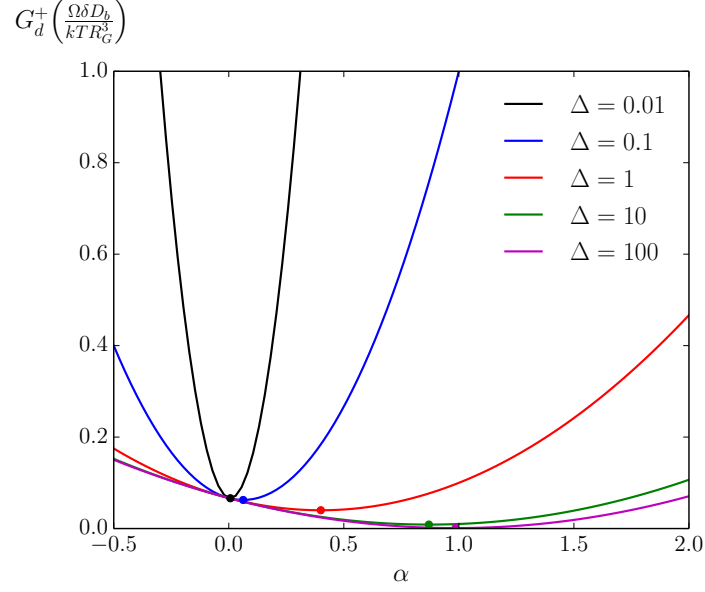


Figure 3: Diffusion contribution to the upper bound on the shear viscosity as a function of parameter α , for different values of the ratio $\Delta = D_l R_G / \delta D_b$. The optimal value of α , leading to the lowest upper bound, is indicated by a circle for each value of Δ .

boundary conditions at the grain boundary and based their analysis on the concept of Somigliana's dislocations. Compared to these authors, our result for G_{sl}^+ is however larger by a factor of two. The reason is that Onaka et al. did not consider the factor $1/2$ in front of the surface integral in Eq. (30). If grain boundary friction is neglected ($\eta = 0$), the result (46) also recovers Herring's result:

$$G_{\text{Herring}} = \frac{1}{10} \frac{k T R_G^2}{\Omega D_l}, \quad (47)$$

(cf. Eq. (11) of (Herring, 1950)). Herring considered the problem of a spherical grain subject to affine velocity boundary conditions and represented the stress using spherical harmonics.

When $\Delta \ll 1$, lattice diffusion is negligible relative to grain boundary diffusion and the viscosity reduces to:

$$G_b^+ = \frac{k T R_G^3}{\Omega \delta D_b} \left(\frac{1}{15} + \frac{3}{5} \eta_b \right), \quad (48)$$

with $\eta_b = \eta \left(\frac{\Omega \delta D_b}{k T R_G^2} \right) = \eta_l / \Delta$. With respect to the result of Onaka et al. (2001), our result for G_b^+ is larger by a factor of two, for the same reason as mentioned below Eq. (46). If we further neglect grain boundary friction ($\eta = 0$), our result is close to the results of Coble who, via some approximations, obtained (cf. Eqs (13) and (14) of (Coble, 1963)):

$$G_{\text{Coble}} = \frac{8}{3} \frac{\pi}{148} \frac{k T}{\Omega \delta D_b} R_G^3 = \frac{1}{17.7} \frac{k T}{\Omega \delta D_b} R_G^3. \quad (49)$$

In Appendix B.1 we show that the trial fields (35)-(38) with optimal parameters (44) constitute an exact solution to the boundary-value problem of a single spherical grain subject to prescribed interface velocity discontinuity of the form (32)-(33), in the sense

that it is possible to calculate corresponding fields of diffusion potential and stress that satisfy all the constitutive and equilibrium equations in the grain. It is also verified in Appendix B.1 that the macroscopic deviatoric stress calculated from the shear viscosity (45) as $\mathbf{S}' = 2G^+ \dot{\mathbf{E}}$ coincides with the macroscopic deviatoric stress calculated by integrating the surface tractions according to Eq. (11).

4.2. Statical bound

We next consider the case of a prescribed deviatoric macroscopic stress of the form:

$$\mathbf{S} = \begin{pmatrix} -\frac{S}{2} & 0 & 0 \\ 0 & -\frac{S}{2} & 0 \\ 0 & 0 & S \end{pmatrix}, \quad (50)$$

and seek to find lower bounds on the shear viscosity using the statical variational principle (Section 3.2). Lower bounds on the shear viscosity are obtained from the potential Φ given by Eq. (23), which for the spherical unit cell is calculated as:

$$\begin{aligned} \Phi = & \frac{1}{V_G} \int_V \frac{1}{2} \frac{D_l}{\Omega k T} \nabla \mu \cdot \nabla \mu \, dV + \frac{1}{2V_G} \int_{A_G} \frac{1}{2} \frac{\delta D_b}{\Omega k T} \nabla_s \mu \cdot \nabla_s \mu \, dA \\ & + \frac{1}{2V_G} \int_{A_G} \frac{1}{2\eta} \sigma_t^2 \, dA, \end{aligned} \quad (51)$$

where μ and σ_t are admissible diffusion potential and tangential stress fields in equilibrium with the macroscopic stress. According to Eq. (25), the lower bound on the shear modulus for the macroscopic loading (50) is given by:

$$G^- = \frac{3S^2}{8\Phi}. \quad (52)$$

We consider a uniform trial stress within the grain, so that the traction field on the grain surface is simply given by:

$$T_i = S_{ij} n_j. \quad (53)$$

Normal and tangent components of \mathbf{T} are calculated as:

$$T_n = \mathbf{T} \cdot \mathbf{n} = \sigma_n = \frac{3S}{4} \left(\cos 2\theta + \frac{1}{3} \right) \quad (54)$$

and

$$T_t = \mathbf{T} \cdot \mathbf{t}_\theta = \sigma_t = -\frac{3}{4} S \sin 2\theta. \quad (55)$$

The normal traction on the boundary in turn sets the trial field of diffusion potential on the boundary: $\mu = -\Omega \sigma_n = -\Omega T_n$. The choice (54)-(55) thus fully specifies the contributions of grain boundary diffusion and sliding to the potential Φ in Eq. (51). On the other hand, an admissible trial diffusion potential field within the bulk should ensure continuity of the diffusion potential, i.e. it should be such that: $\mu(R_G, \theta) = -\frac{3}{4} \Omega S (\cos 2\theta + \frac{1}{3})$ and $\frac{\partial \mu}{\partial \theta}(R_G, \theta) = \frac{3}{2} \Omega S \sin 2\theta$. A parametrised set of trial fields satisfying these two conditions is given by:

$$\mu(r, \theta) = \frac{3}{2} \frac{\Omega S}{R_G^2} r^2 \left(-\frac{1}{2} \cos 2\theta + \gamma \right) - \frac{3}{2} \Omega S \left(\gamma + \frac{1}{6} \right), \quad (56)$$

where γ is an adjustable parameter. In the bulk, the gradient of the trial field of diffusion potential (56) is calculated as:

$$\nabla_r \mu = 3 \frac{\Omega S r}{R_G^2} \left(-\frac{1}{2} \cos 2\theta + \gamma \right) \quad (57)$$

$$\nabla_\theta \mu = \frac{3}{2} \frac{\Omega S r}{R_G^2} \sin 2\theta. \quad (58)$$

The functional Φ in Eq. (51) is then calculated as:

$$\Phi = \frac{\Omega \delta D_b}{k T R_G^3} S^2 \left(\frac{9}{10} + \frac{27}{40} \Delta \left(1 + 4\gamma^2 + \frac{4\gamma}{3} \right) + \frac{9}{40} \frac{1}{\eta_b} \right). \quad (59)$$

Lower bounds on the shear viscosity then follow from Eq. (52):

$$G^- = \frac{k T R_G^3}{\Omega \delta D_b} \left(\frac{12}{5} + \frac{9}{5} \Delta \left(1 + 4\gamma^2 + \frac{4\gamma}{3} \right) + \frac{3}{5} \frac{1}{\eta_b} \right)^{-1}. \quad (60)$$

The optimal (i.e. highest) lower bound is obtained by finding the value of the parameter γ that minimises the potential Φ given by Eq. (59). This leads to

$$\gamma = -\frac{1}{6}. \quad (61)$$

The evolution of the lower bound for G (60) as a function of the parameter γ is illustrated in Fig. 4, for $\eta_l = 0.2$. The optimal value of γ , leading to the highest lower bound, is indicated by a circle on the figure.

For the optimal choice (61), the potential reduces to:

$$\Phi = \frac{\Omega \delta D_b}{k T} \frac{S^2}{R_G^3} \left(\frac{2}{5} + \frac{4}{15} \Delta + \frac{1}{10} \frac{1}{\eta_b} \right), \quad (62)$$

and the corresponding optimal lower bound is given by:

$$G^- = \frac{k T R_G^3}{\Omega \delta D_b} \left(\frac{12}{5} + \frac{8}{5} \Delta + \frac{3}{5} \frac{1}{\eta_b} \right)^{-1}. \quad (63)$$

In the limit where grain boundary diffusion is negligible relative to lattice diffusion, $\Delta \ll 1$ and shear viscosity is dominated by lattice diffusion and grain boundary sliding:

$$G_l^- = \frac{k T R_G^2}{\Omega D_l} \left(\frac{8}{5} + \frac{3}{5 \eta_l} \right)^{-1}. \quad (64)$$

In the limit where lattice diffusion is negligible relative to grain boundary diffusion, $\Delta \gg 1$ and shear viscosity is dominated by grain boundary diffusion and sliding:

$$G_b^- = \frac{k T R_G^3}{\Omega \delta D_b} \left(\frac{12}{5} + \frac{3}{5 \eta_b} \right)^{-1}. \quad (65)$$

In Appendix B.2, we show that the trial field of diffusion potential corresponding to the optimal value (61) of the parameter γ is an exact solution to the boundary-value problem of a single spherical grain subject to prescribed tractions of the form (53), in the sense that it is possible to calculate lattice and grain-boundary diffusion fluxes that satisfy the constitutive relations and such that the lattice diffusion flux is divergence-free in the grain interior.

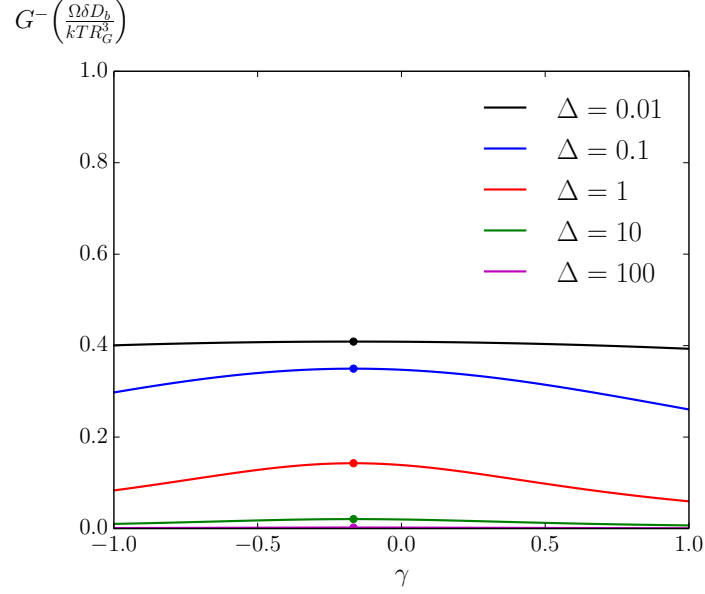


Figure 4: Lower bound on the shear viscosity as a function of parameter γ , for $\eta_l = 0.2$ and different values of the ratio $\Delta = D_l R_G / \delta D_b$. The optimal value of γ , leading to the highest lower bound, is indicated by a circle for each value of Δ .

Table 1: Effective shear viscosity G in the lattice diffusion-dominated ($D_l R_G \gg \delta D_b$) and grain boundary diffusion-dominated ($D_l R_G \ll \delta D_b$) regimes, as predicted by different models.

	$D_l R_G \gg \delta D_b$	$D_l R_G \ll \delta D_b$
Upper bound	$\frac{1}{10} \frac{kTR_G^2}{\Omega D_l} + \frac{3}{5} \eta R_G$	$\frac{1}{15} \frac{kTR_G^3}{\Omega \delta D_b} + \frac{3}{5} \eta R_G$
Lower bound	$\left(\frac{8}{5} \frac{\Omega D_l}{kTR_G^2} + \frac{3}{5\eta R_G} \right)^{-1}$	$\left(\frac{12}{5} \frac{\Omega \delta D_b}{kTR^3} + \frac{3}{5\eta R_G} \right)^{-1}$
Herring (1951)	$\frac{1}{10} \frac{kTR_G^2}{\Omega D_l}$	
Coble (1963)		$\frac{1}{17.7} \frac{kTR_G^3}{\Omega \delta D_b}$

5. Discussion

In the previous section, we used kinematic and statical variational principles to identify optimal upper and lower bounds on the shear viscosity of random aggregates represented by the spherical unit cell model. These optimal bounds were further shown to correspond to exact solutions of the boundary-value problem of a single spherical grain subject respectively to affine velocity jumps or uniform tractions on the grain boundary surface. Because of the spherical grain shape and simplified representation of grain-to-grain interactions through point contacts randomly distributed on the sphere surface, compatibility of velocity jumps and equilibrium of surface tractions across grain boundaries are also automatically fulfilled. In contrast, in a realistic random geometry of faceted grains, stresses corresponding to affine trial velocity jumps would not be equilibrated. Conversely, velocity and diffusion flux fields corresponding to uniform stress trial fields would not satisfy compatibility of deformation and conservation of mass. This is analogous to Voigt and Reuss bounds on the elastic modulus of heterogeneous media.

As illustrated below, the modulus corresponding to the spherical grain subject to affine velocity jump, Eq. (45) is larger or equal to the modulus corresponding to the spherical

grain subject to uniform traction boundary condition, Eq. (63). This is consistent with the result established in Appendix A.2. The existence of two distinct values of the effective shear viscosity indicates that the spherical unit cell model does not constitute a RVE of the aggregate. Indeed, by definition, the effective behaviour of a RVE should be independent of whether macroscopic stress or macroscopic strain is prescribed. Mechanical analysis on a proper RVE is needed to assess whether a mean estimate between these two results would constitute an accurate estimate of the actual response of random aggregates of faceted grains.

A summary of our results in the two limiting regimes (lattice diffusion-dominated and grain boundary diffusion-dominated regimes) is presented in Table 1. Figure 5 shows normalised optimal upper and lower bounds on the shear viscosity drawn from Eqs (46) and (64) (lattice diffusion-dominated, Fig. 5a) or Eqs (48) and (65) (grain boundary diffusion-dominated, Fig. 5b) as a function of the dimensionless friction parameters η_l or η_b . Note in particular that η_l or η_b increase when grain size decrease. Also note the different normalisation used for both the friction coefficient and the viscosity in terms of powers of R_G . η_l or η_b can be interpreted as the ratio of a characteristic time for grain boundary sliding $\tau_{sl} = \frac{\eta \Omega R_G}{kT}$ (i.e. the timescale for relaxation of tangential stresses under an applied strain in the absence of diffusion) to a characteristic time for diffusion in the lattice, $\tau_l = \frac{R_G^2}{D_l}$, or along grain boundaries, $\tau_b = \frac{R_G}{\delta} \frac{R_G^2}{D_b}$.

As lattice diffusion dominates at large R_G , a decrease of R_G brings about a transition from Fig. 5a to Fig. 5b around $R_G = \delta \frac{D_b}{D_l}$, for which $\tau_l = \tau_b$. This threshold also corresponds to $\eta_l = \eta_b$, which depends on the material properties. For example, if $\delta \frac{D_b}{D_l} = 10^{-6}$ m, the threshold occurs at $R_G = 1$ μm , and if $\eta \frac{\Omega D_l}{kT} = 10^{-7}$ m, it corresponds to $\eta_l = \eta_b = 0.1$: the relevant parts of the curves are then the range $\eta_l < 0.1$ in Fig. 5a and the range $\eta_b > 0.1$ in Fig. 5b. The threshold corresponding to $R_G = 1$ μm moves to the right if η is larger. Reliable experimental data on the value to be postulated for the grain boundary friction coefficient η in polycrystals are very scarce. As mentioned in the Introduction, arguments linked to the mechanisms of climb and glide of GBDs suggest that, for common grain sizes, $\eta_l \ll 1$ and $\eta_b \ll 1$. Nonetheless, η_l and η_b can become large in nanomaterials. As an example, from creep tests on ZrO_2 at 1400°C under 3 MPa, Kim et al. (Kim et al., 2004) estimated $\eta_b \approx 0.5$ for ZrO_2 when $R_G = 0.35$ μm (on the basis of a two-dimensional model assuming a regular hexagonal lattice of grains). Hence, the range of scale chosen for the abscissae in Fig. 5 can be considered relevant for nanostructured materials.

For a fixed grain size, upper and lower bounds both monotonically increase with η . In Fig. 5a, the upper bound coincides with Herring's result for $\eta_l = 0$ and increases linearly with η_l with a slope of $3/5$. In Fig. 5b, the upper bound is close to Coble's result for $\eta_b = 0$ and increases with the same slope. This follows from the kinematic approach, according to which the tangential velocity is prescribed, and the contribution of grain boundary sliding to macroscopic stress scales linearly with the friction coefficient. In contrast, the lower bound is a non-linear function of the friction coefficient, with $G_l^- = G_b^- = 0$ for $\eta_l = \eta_b = 0$ and $G_l^- = \frac{5}{8} \frac{kT R_G^2}{\Omega D_l}$ or $G_b^- = \frac{5}{12} \frac{kT R_G^3}{\Omega \delta D_l}$ when η_l or $\eta_b \rightarrow \infty$. These two limits respectively correspond to infinite and zero tangential velocity discontinuity at the grain boundary under prescribed tangential stress. The uncertainty on the mean estimate between the bounds is particularly large when η_l or η_b tend to zero (if $\eta \neq 0$, a domain of dominance of lattice diffusion always prevails below a certain threshold).

Interestingly, there is a particular value of the friction coefficient at which the curves

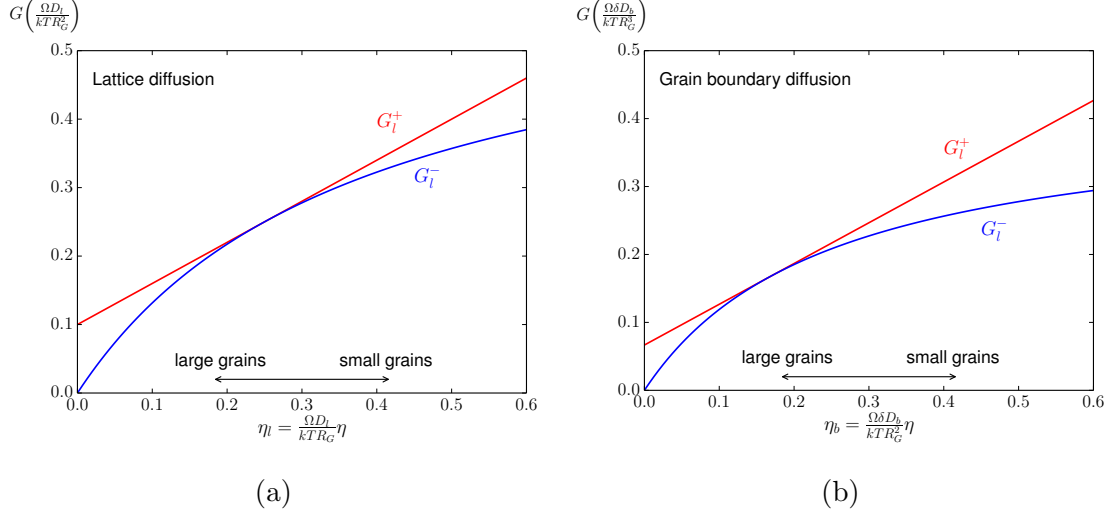


Figure 5: (a) Bounds on the shear viscosity drawn from Eqs (46) and (64). (b) Bounds on the shear viscosity drawn from Eqs (48) and (65).

for the two bounds are tangent to one another:

$$G_l^+ = G_l^- = \frac{1}{4} \frac{kTR_G^2}{\Omega D_l} = \frac{5}{2} (G_l^+)_{\eta=0} = \eta R_G \quad (66)$$

when $\eta_l = \frac{1}{4}$, and

$$G_b^+ = G_b^- = \frac{1}{6} \frac{kTR_G^3}{\Omega \delta D_b} = \frac{5}{2} (G_b^+)_{\eta_b=0} = \eta R_G \quad (67)$$

when $\eta_b = \frac{1}{6}$. The condition for the tangency of the curves is discussed in Appendix C. It is shown that there is a particular value of η for which the traction field calculated when boundary velocity jumps are prescribed by macroscopic strain rate is identical to the traction field corresponding to prescribed uniform tractions, and vice versa. For that particular value of η , the affine relation (31) between velocity and macroscopic strain rate and the uniform traction condition (53) hold simultaneously. The velocity jump vectors and traction vectors are then parallel to each other, and the shear viscosity is $G = \eta R_G$, independent of the value of other material coefficients. The particular value (66) coincides with the "unrelaxed" solution obtained by Herring by simultaneously assuming uniform stress and strain rate within the grain (see Eq. (7) in (Herring, 1950)). For steady-state creep, our results show that this particular solution can be recovered for a particular value of the friction coefficient η .

We investigate the scaling of the shear viscosity with grain size by fitting Eqs (46), (64), (48) and (65) with a power law in terms of the grain size. Specifically, the dependence on η_l or η_b of the apparent grain size sensitivity exponent p was calculated via the relationship

$$p_l^+ = \frac{d \ln G_l^+}{d \ln R_G} = \frac{d G_l^+}{d R_G} \frac{R_G}{G_l^+} \quad (68)$$

and the like for the other bounds. The results are presented in Fig. 6. For zero grain boundary friction, G_l^+ scales with the square of the grain size (Herring's result), whereas G_b^+ scales with the third power of the grain size (Coble's result). In the limit of high η_l or η_b , the upper bound is dominated by grain boundary sliding and scaling exponent p tends

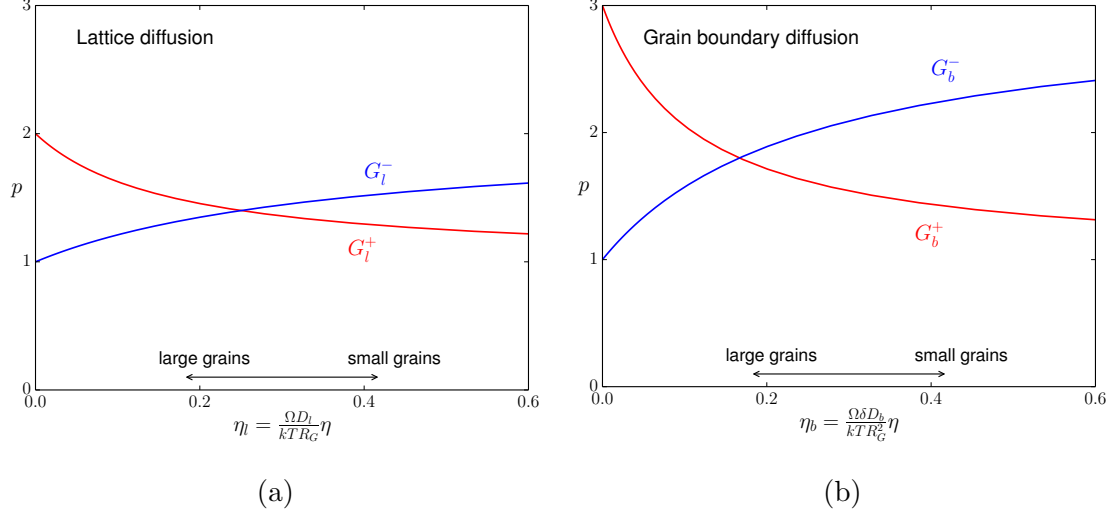


Figure 6: (a) Grain size sensitivity exponent of the bounds (46) and (64). (b) Grain size sensitivity exponent of the bounds (48) and (65).

to 1. In the same limit, sliding becomes effectively inoperative in the lower bound and the scaling exponent tends to 2 or 3. The mean between the two curves varies in the ranges $1.5 \geq p_l \geq 1.4$ and $2 \geq p_b \geq 1.8$. These curves cast doubt on the validity of the method of identification of the dominant creep mechanism based on the grain size dependence of creep rate: dominance of lattice diffusion if $p = 2$; dominance of grain boundary diffusion if $p = 3$; dominance of grain boundary friction forces if $p = 1$. Experimentally, p values close to 2 were much more frequently reported than p values close to 3 (Coble, 1963; Cannon and Sherby, 1977; Cannon and Langdon, 1988; Mishra et al., 1988; Wang, 2000; Ruano et al., 2003).

In the literature, most experimental studies of creep under low stress reported creep rates significantly higher than the predictions of Herring's and Coble's models (Cannon and Sherby, 1977; Cannon and Langdon, 1988; Mishra et al., 1988; Wang, 2000). It may be tempting to link this discrepancy to the outcomes of the present work showing that classical models provide only an upper bound for shear viscosity and that the lower bound may be very low if the friction coefficient η is small. Unfortunately, very little is known today about the value to be ascribed to η . In addition, in many cases, microstructural observations after creep testing or after superplastic straining showed evidence of the occurrence of Rachinger sliding (usually referred to as "grain boundary sliding (GBS)") (Wang, 2000; Chokshi, 2002; Ruano et al., 2003). Meaningful comparison with experimental creep data then requires a model involving the possibility of a strain contribution due to GBS. Forthcoming work will aim at addressing this issue as well as the effect of grain shape anisotropy and the difference between the present model and previous models based on periodic lattices of grains in two- or three-dimension (Gibbs, 1966; Raj and Ashby, 1971; Beere, 1976, 1978; Spingarn and Nix, 1978; Greenwood, 1985, 1992; Burton, 1994; Kim et al., 2003, 2004).

6. Conclusion

By revisiting classical models for NHC creep under the light of variational principles, the present work reveals that the widely acknowledged Herring's and Coble's predictions

for viscosity dominated by lattice and/or grain boundary diffusion are actually upper bounds arising from the use of affine trial velocity discontinuity at interfaces, and that conversely lower bounds can be accessed via the use of uniform trial stresses in the grains. To the best of our knowledge these lower bounds have not been identified earlier in the literature. If the grain is represented by a sphere, the lowest upper bound and the highest lower bound are two independent exact solutions of the governing equations within the grain. The existence of such bounds challenges the validity of the classical method of identification of the dominant creep mechanism from the grain size sensitivity exponent. The work also emphasizes the role of grain boundary friction in diffusional viscosity.

Appendix A. Variational formulations of the boundary-value problem

Appendix A.1. Principle of virtual powers

Consider a polycrystalline aggregate occupying a volume V with external surface A . The aggregate is subject to prescribed traction \mathbf{T} on A_T , and to prescribed velocity $\bar{\mathbf{v}}$ on A_V , with $A_T \cup A_V = A$ and $A_T \cap A_V = \emptyset$. Let σ_n^* and σ_t^* be normal and tangential interface stresses in equilibrium with traction \mathbf{T}^* on the external surface. Let Δv_n^c and Δv_t^c be normal and tangential interface velocity jumps kinematically compatible with velocity \mathbf{v}^c on the external surface. The Principle of Virtual Powers expresses as (Needleman and Rice, 1980; McMeeking and Kuhn, 1992; Cocks, 1996):

$$\int_A \mathbf{T}^* \cdot \mathbf{v}^c dA = \int_{A_b} (\sigma_n^* \Delta v_n^c + \sigma_t^* \Delta v_t^c) dA. \quad (69)$$

Using the divergence theorem together with relations (3), (4), (6) and (7), Eq. (69) can be rewritten as:

$$\int_A \mathbf{T}^* \cdot \mathbf{v}^c dA = \int_V -\frac{\mathbf{j}_l^c}{\Omega} \cdot \nabla \mu^* dV + \int_{A_b} \left(-\frac{\mathbf{j}_b^c}{\Omega} \cdot \nabla_s \mu^* + \sigma_t^* \Delta v_t^c \right) dA. \quad (70)$$

In this expression, $\mu^* = -\Omega \sigma_n^*$ on A_b , and \mathbf{j}_l^c and \mathbf{j}_b^c are related to Δv_n^c by Eq. (7) on A_b , with $\nabla \cdot \mathbf{j}_l^c = 0$ in the grain interior. We have also assumed that the net fluxes ($\mathbf{j}_l^c \cdot \mathbf{n}$) and ($\mathbf{j}_b^c \cdot \mathbf{n}$) vanish on the external surface.

Following Cocks (1996), let us identify the traction \mathbf{T}^* , stress σ_t^* and diffusion potential μ^* in Eq. (70) with the exact fields, and identify the compatible fields of velocity \mathbf{v}^c , diffusion fluxes \mathbf{j}_l^c and \mathbf{j}_b^c , and velocity jump Δv_t^c with small perturbations $\delta \mathbf{v}$, $\delta \mathbf{j}_l$, $\delta \mathbf{j}_b$ and $\delta \Delta v_t$ about the exact solution. In particular, the perturbation $\delta \mathbf{v}$ vanishes on A_V . Then, relation (70) becomes:

$$V \delta I \equiv \int_V \frac{kT}{\Omega D_l} \mathbf{j}_l \cdot \delta \mathbf{j}_l dV + \int_{A_b} \left(\frac{kT}{\Omega \delta D_b} \mathbf{j}_b \cdot \delta \mathbf{j}_b + \eta \Delta v_t \delta \Delta v_t \right) dA - \int_{A_T} \bar{\mathbf{T}} \cdot \delta \mathbf{v} = 0, \quad (71)$$

where we have also used the constitutive relations (2), (5) and (8). This expression shows that the functional I defined by Eq. (18) is stationary for the exact fields. It can also be shown that the stationary point corresponds to a minimum, see McMeeking and Kuhn (1992) for the proof. In the particular case where $A = A_V$ and $A_T = \emptyset$, evaluating the principle of virtual powers (70) for the exact fields also gives the following equality:

$$\int_A \mathbf{T} \cdot \bar{\mathbf{v}} dA = \int_V \frac{kT}{\Omega D_l} \mathbf{j}_l \cdot \mathbf{j}_l dV + \int_{A_b} \left(\frac{kT}{\Omega \delta D_b} \mathbf{j}_b \cdot \mathbf{j}_b + \eta (\Delta v_t)^2 \right) dA = 2V \Psi. \quad (72)$$

Let us now identify the compatible velocity and diffusion fluxes in Eq. (70) with the exact fields, and identify the equilibrated fields of traction, stress and diffusion potential with small perturbations $\delta \mathbf{T}$, $\delta \mu$, and $\delta \sigma_t$ about the exact solution. In particular, the perturbation $\delta \mathbf{T}$ vanishes on A_T . Then, relation (70) yields:

$$V \delta J \equiv \int_V \frac{D_l}{\Omega k T} \nabla \mu \cdot \delta \nabla \mu dV + \int_{A_b} \left(\frac{\delta D_b}{\Omega k T} \nabla \mu_s \cdot \delta \nabla \mu_s + \frac{\sigma_t}{\eta} \delta \sigma_t \right) dA - \int_{A_V} \bar{\mathbf{v}} \cdot \delta \mathbf{T} = 0, \quad (73)$$

where we have used the constitutive relations (2), (5) and (8). This expression shows that the functional J defined by Eq. (22) is stationary for the exact fields. It can also be shown that the stationary point corresponds to a minimum. In the particular case where $A = A_T$ and $A_V = \emptyset$, evaluating the principle of virtual powers (70) for the exact fields gives the following equality:

$$\int_A \mathbf{T} \cdot \bar{\mathbf{v}} dA = \int_V \frac{D_l}{\Omega k T} \nabla \mu \cdot \nabla \mu dV + \int_{A_b} \left(\frac{\delta D_b}{\Omega k T} \nabla_s \mu \cdot \nabla_s \mu + \frac{\sigma_t^2}{\eta} \right) dA = 2V\Phi. \quad (74)$$

It can further be shown that $I + J = 0$ for the exact fields. From Eqs (18) and (22), direct calculation gives:

$$\begin{aligned} V(I + J) &= \frac{1}{2} \int_V \frac{kT}{\Omega D_l} \dot{\mathbf{j}}_l \cdot \dot{\mathbf{j}}_l dV + \frac{1}{2} \int_{A_b} \left(\frac{kT}{\Omega \delta D_b} \dot{\mathbf{j}}_b \cdot \dot{\mathbf{j}}_b + \eta (\Delta v_t)^2 \right) dA \\ &\quad + \frac{1}{2} \int_V \frac{D_l}{\Omega k T} \nabla \mu \cdot \nabla \mu dV + \frac{1}{2} \int_{A_b} \left(\frac{\delta D_b}{\Omega k T} \nabla_s \mu \cdot \nabla_s \mu + \frac{\sigma_t^2}{\eta} \right) dA \\ &\quad - \int_{A_F} \bar{\mathbf{T}} \cdot \mathbf{v} dA - \int_{A_V} \mathbf{T} \cdot \bar{\mathbf{v}} dA. \end{aligned} \quad (75)$$

Using the constitutive relations (2), (5) and (8), the latter equation becomes:

$$V(I + J) = \int_V -\frac{\dot{\mathbf{j}}_l}{\Omega} \cdot \nabla \mu dV + \int_{A_b} \left(-\frac{\dot{\mathbf{j}}_b}{\Omega} \cdot \nabla_s \mu + \sigma_t \Delta v_t \right) dA - \int_A \mathbf{T} \cdot \mathbf{v} dA, \quad (76)$$

which vanishes by virtue of the principle of virtual powers (70) calculated for the exact fields. It also follows that $\Psi + \Phi = \frac{1}{V} \int_A \mathbf{T} \cdot \mathbf{v} dS = \mathbf{S} : \dot{\mathbf{E}}$, where the last equality follows from Hill's condition (13).

Appendix A.2. Comparison of the effective moduli for affine and uniform traction boundary conditions

We use the variational principles to show that the effective shear modulus for an aggregate subject to affine velocity boundary conditions is larger or equal to the modulus of the same aggregate subject to uniform traction boundary conditions. The proof follows Huet (1990), who demonstrated the analogous result in the context of elastic heterogeneous media.

Let us consider two distinct boundary-value problems for the same aggregate:

1. Problem 1: the aggregate is subject to affine boundary conditions of the form $\mathbf{v}_1 = \dot{\mathbf{E}}_1 \cdot \mathbf{x}$ on A . Solution fields for this problem are written \mathbf{v}_1 , $\dot{\mathbf{j}}_{l1}$, $\dot{\mathbf{j}}_{b1}$, σ_1 , and μ_1 .
2. Problem 2: the aggregate is subject to uniform traction boundary conditions of the form $\mathbf{T} = \mathbf{S}_2 \cdot \mathbf{n}$ on A . Solution fields for this problem are written \mathbf{v}_2 , $\dot{\mathbf{j}}_{l2}$, $\dot{\mathbf{j}}_{b2}$, σ_2 and μ_2 .

Using the fields $\boldsymbol{\sigma}_2$ and μ_2 as admissible fields in the statical variational formulation of Problem 1 (section 3.2), we have the following inequality:

$$-J_1[\boldsymbol{\sigma}_2, \mu_2] \leq -J_1[\boldsymbol{\sigma}_1, \mu_1] = I_1[\mathbf{v}_1, \mathbf{j}_{l1}, \mathbf{j}_{b1}], \quad (77)$$

where we also used the result $I_1 + J_1 = 0$ for the exact fields of Problem 1. From the definition (22) of the functional J , the left-hand side of Eq. (77) can be rewritten as:

$$\begin{aligned} -J_1[\boldsymbol{\sigma}_2, \mu_2] &= -\frac{1}{V} \left[\int_V \frac{1}{2} \frac{D_l}{\Omega k T} \boldsymbol{\nabla} \mu_2 \cdot \boldsymbol{\nabla} \mu_2 dV \right. \\ &\quad \left. + \int_{A_b} \left(\frac{1}{2} \frac{\delta D_b}{\Omega k T} \boldsymbol{\nabla}_s \mu_2 \cdot \boldsymbol{\nabla}_s \mu_2 + \frac{\sigma_{t2}^2}{2\eta} \right) dA - \int_A (\mathbf{S}_2 \cdot \mathbf{n}) \cdot \mathbf{v}_1 dA \right] \\ &= -\Phi_2[\boldsymbol{\sigma}_2, \mu_2] + \mathbf{S}_2 : \dot{\mathbf{E}}_1 \\ &= -\frac{\mathbf{S}_2 : \mathbf{S}_2}{4G_2} + \mathbf{S}_2 : \dot{\mathbf{E}}_1, \end{aligned} \quad (78)$$

where we also used Eq. (9) and (24). In the latter equation, G_2 is the effective shear modulus for Problem 2. On the other hand, the right-hand side of Eq. (78) can be expressed as:

$$I_1[\mathbf{v}_1, \mathbf{j}_{l1}, \mathbf{j}_{b1}] = \Psi_1[\mathbf{v}_1, \mathbf{j}_{l1}, \mathbf{j}_{b1}] = G_1 \dot{\mathbf{E}}_1 : \dot{\mathbf{E}}_1, \quad (79)$$

with G_1 the effective shear modulus for Problem 1. Inserting Eqs (78) and (79) into Eq. (77) gives the inequality:

$$-\frac{\mathbf{S}_2 : \mathbf{S}_2}{4G_2} + \mathbf{S}_2 : \dot{\mathbf{E}}_1 \leq G_1 \dot{\mathbf{E}}_1 : \dot{\mathbf{E}}_1. \quad (80)$$

For a fixed value of $\dot{\mathbf{E}}_1$, it is easily verified that the left-hand side of the above inequality reaches a maximum for $\mathbf{S}_2 = 2G_2 \dot{\mathbf{E}}_1$ (i.e. when the applied macroscopic stress for Problem 2 coincides with the macroscopic stress in Problem 1). For this particular value of \mathbf{S}_2 , the inequality (80) becomes:

$$G_2 \dot{\mathbf{E}}_1 : \dot{\mathbf{E}}_1 \leq G_1 \dot{\mathbf{E}}_1 : \dot{\mathbf{E}}_1. \quad (81)$$

This shows that the shear modulus of an aggregate subject to uniform traction boundary conditions is lower or equal to the modulus of the same aggregate subject to affine velocity boundary conditions. The equality holds when the relationship between macroscopic stress and strain rate does not depend on the type of the boundary conditions, which is expected to occur when the aggregate is sufficiently large (i.e. contains a sufficiently large number of grains) and is statistically representative.

Appendix B. Exact solutions of the boundary-value problem for a spherical grain

Appendix B.1. Prescribed velocity jump at grain boundary

Using the optimal parameters (44), the diffusion flux field in the bulk lattice (35)-(36) becomes:

$$j_{lr}(r, \theta) = \frac{3}{4} \left(1 + \frac{3}{2\Delta} \right)^{-1} r \dot{E} \left(\cos 2\theta + \frac{1}{3} \right) \quad (82)$$

$$j_{l\theta}(r, \theta) = -\frac{3}{4} \left(1 + \frac{3}{2\Delta} \right)^{-1} r \dot{E} \sin 2\theta, \quad (83)$$

589 and the surface flux (38) along the grain boundary becomes:

$$j_{b\theta} = -\frac{1}{2} \left(1 + \frac{2\Delta}{3}\right)^{-1} R_G^2 \dot{E} \sin 2\theta. \quad (84)$$

590 The diffusion potential in the bulk lattice is obtained by integrating Eqs (82)-(83):

$$\mu(r, \theta) = -\frac{3}{8} \frac{kT}{D_l} \left(1 + \frac{3}{2\Delta}\right)^{-1} r^2 \dot{E} \left(\cos 2\theta + \frac{1}{3}\right) + C_1, \quad (85)$$

591 where C_1 is an integration constant. Integration of Eq. (84) along the grain boundary
592 provides the following expression of the diffusion potential on the surface:

$$\mu(\theta) = -\frac{1}{4} \frac{kT}{\delta D_b} \left(1 + \frac{2\Delta}{3}\right)^{-1} R_G^3 \dot{E} \cos 2\theta + C_2, \quad (86)$$

593 where C_2 is another integration constant. Continuity of the diffusion potential at the
594 grain boundary requires the two integration constants to be related by:

$$C_2 = -\frac{1}{8} \left(1 + \frac{3}{2\Delta}\right)^{-1} R_G^2 \dot{E} \frac{kT}{D_l} + C_1. \quad (87)$$

595 Thus, the diffusion potential is only known up to an integration constant, which can be
596 chosen arbitrarily. As we show below, the choice of the integration constants sets the
597 value of the mean macroscopic stress. The optimal choice of parameters (44) is actually
598 the only one for which continuity of diffusion potential on the boundary can be enforced.

599 In terms of C_2 , the normal stress on the boundary, $\sigma_n = -\mu/\Omega$ is given by:

$$\sigma_n = \frac{1}{4} \frac{kT}{\Omega \delta D_b} R_G^3 \dot{E} \left(1 + \frac{2\Delta}{3}\right)^{-1} \cos 2\theta + S_0, \quad (88)$$

600 where $S_0 = -C_2/\Omega$. On the other hand, the tangential stress is obtained from Eqs (8)
601 and (33) as:

$$\sigma_t = -\frac{3}{2} \eta R_G \dot{E} \sin 2\theta. \quad (89)$$

602 Eqs (88)-(89) set the traction vector on the grain boundary. For any choice of S_0 , it
603 is always possible to find a field of stress within the grain that satisfies the equilibrium
604 equation $\nabla \cdot \boldsymbol{\sigma} = \mathbf{0}$ and that is compatible with the boundary traction.

605 The macroscopic stress can be calculated from the interface stresses (88)-(89) using
606 Eq. (11), giving

$$S_{11} = S_{22} = -\frac{3}{20} \left(1 + \frac{2\Delta}{3}\right)^{-1} \frac{kT R_G^3 \dot{E}}{\Omega \delta D_b} - \frac{1}{5} \eta R \dot{E} + S_0, \quad (90)$$

$$S_{33} = \frac{1}{20} \left(1 + \frac{2\Delta}{3}\right)^{-1} \frac{kT R_G^3 \dot{E}}{\Omega \delta D_b} + \frac{2}{5} \eta R \dot{E} + S_0 \quad (91)$$

607 and the mean macroscopic stress is given by:

$$S_m = -\frac{1}{12} \left(1 + \frac{2\Delta}{3}\right)^{-1} \frac{kT R_G^3 \dot{E}}{\Omega \Delta D_b} + S_0. \quad (92)$$

It can be verified that the deviatoric macroscopic stress $S'_{ij} = S_{ij} - S_m \delta_{ij}$ obtained from Eqs (90)-(91) coincides with the macroscopic deviatoric stress calculated from the viscosity, $S'_{ij} = 2G^+ \dot{E}_{ij}$, with G^+ given by Eq. (45), regardless of the choice of S_0 .

One can always choose the constant S_0 such that the macroscopic mean stress vanishes and $\mathbf{S} = \mathbf{S}'$:

$$S_0 = \frac{1}{12} \left(1 + \frac{2\Delta}{3} \right)^{-1} \frac{kTR_G^3 \dot{E}}{\Omega \Delta D_b}. \quad (93)$$

For this choice of S_0 , the interface stresses (88)-(89) particularise as:

$$\sigma_n = \frac{1}{4} \frac{kTR_G^3 \dot{E}}{\Omega \delta D_b} \left(1 + \frac{2\Delta}{3} \right)^{-1} \left(\cos 2\theta + \frac{1}{3} \right), \quad (94)$$

$$\sigma_t = -\frac{3}{2} \eta R_G \dot{E} \sin 2\theta. \quad (95)$$

Note that the choice of S_0 does not affect the tangential stress due to sliding, whose contribution to the macroscopic stress is always purely deviatoric.

Appendix B.2. Prescribed tractions at grain boundary

Using the optimal value (61) of parameter γ , the diffusion potential (56) becomes:

$$\mu(r, \theta) = -\frac{3}{4} \frac{\Omega S}{R_G^2} r^2 \left(\cos 2\theta + \frac{1}{3} \right). \quad (96)$$

The optimal value (61) is the only one that ensures that $\nabla^2 \mu = 0$. The corresponding diffusion flux field in the bulk lattice is calculated from the constitutive relation (2):

$$j_{lr}(r, \theta) = \frac{3}{2} \frac{D_l}{kT} \frac{\Omega S}{R_G^2} r \left(\cos 2\theta + \frac{1}{3} \right) \quad (97)$$

$$j_{l\theta}(r, \theta) = -\frac{3}{2} \frac{D_l}{kT} \frac{\Omega S}{R_G^2} r \sin 2\theta, \quad (98)$$

which is divergence-free. The surface flux along the grain boundary is obtained from relation (5):

$$j_{b\theta}(\theta) = -\frac{3}{2} \frac{\delta D_b}{kT} \frac{\Omega S}{R_G} \sin 2\theta. \quad (99)$$

Normal and tangential velocity jumps are respectively calculated from the continuity condition (34) and the constitutive relation (8):

$$\Delta v_n = \frac{9}{2} \frac{\delta D_b}{kT} \frac{\Omega S}{R_G^2} \left(1 + \frac{2\Delta}{3} \right) \left(\cos 2\theta + \frac{1}{3} \right) \quad (100)$$

$$\Delta v_t = -\frac{3}{4} \frac{S}{\eta} \sin 2\theta. \quad (101)$$

The traction field on the grain surface is prescribed by Eq. (53) and corresponds to a uniform stress in the grain. It follows from the above considerations that expression (96) for the diffusion potential is the exact solution of the spherical grain problem under prescribed traction at grain boundary. One can also verify that the macroscopic strain rate obtained by using the latter two equations into Eq. (10) is deviatoric and coincides with the macroscopic strain rate calculated directly from the lower bound, $\dot{E}_{ij} = \frac{S_{ij}}{2G^-}$.

Appendix C. Point of tangency of upper and lower bound curves

By comparing the stresses (94)-(95) under prescribed velocity conditions to the stresses (54)-(55) under prescribed tractions at grain boundary, we find that the two solutions are compatible (i.e., affine velocity jump at the interface and uniform stress within the grain occur simultaneously) only if the following condition is met:

$$\eta = \frac{1}{6} \left(1 + \frac{2\Delta}{3} \right)^{-1} \frac{kTR_G^2}{\Omega\delta D_b}. \quad (102)$$

Conversely, comparison of the velocity jumps (100)-(101) under prescribed tractions to the velocity jumps (32)-(33) under prescribed velocities leads to the exact same condition. It thus follows that the solutions under the two considered loading conditions coincide for the particular value (102) of η , and so does the effective shear viscosity.

Condition (102) can be particularised to the two limit cases:

- Lattice diffusion-dominated ($\Delta \rightarrow \infty$):

$$\eta \frac{\Omega D_l}{kTR_G} = \eta_l = \frac{1}{4}. \quad (103)$$

- Grain boundary diffusion-dominated ($\Delta \rightarrow \infty$):

$$\eta \frac{\Omega\delta D_b}{kTR_G^2} = \eta_b = \frac{1}{6}. \quad (104)$$

It can also be verified that, for the particular value (102) of η , the interface velocity vector and traction vector are parallel, i.e. $\frac{\Delta v_n}{T_n} = \frac{\Delta v_t}{T_t} = \text{constant}$. Here, the constant is set by the friction coefficient itself, according to the model of grain boundary sliding (8):

$$\mathbf{T} = \eta \Delta \mathbf{v}. \quad (105)$$

Using relation (105) into expression (11) of the macroscopic stress, and accounting for expression (10) of the macroscopic strain rate, one directly obtains:

$$S_{ij} = 2R_G\eta\dot{E}_{ij}. \quad (106)$$

The same result is obtained by first inserting relation (105) into expression (10) of the macroscopic strain rate and then identifying the macroscopic stress using Eq. (11). The shear viscosity is thus given by $G = \eta R_G$, independent of the type of boundary condition and the value of other material properties.

References

- Arzt, E., Ashby, M., Verrall, R., 1983. Interface controlled diffusional creep. *Acta Metallurgica* 31, 1977–1989.
- Ashby, M., 1969. On interface-reaction control of Nabarro-Herring creep and sintering. *Scripta Metallurgica* 3, 837–842.
- Ashby, M., 1972. Boundary defects, and atomistic aspects of boundary sliding and diffusional creep. *Surface Science* 31, 498–542.
- Ashby, M., Edward, G., Davenport, J., Verrall, R., 1978. Application of bound theorems for creeping solids and their application to large strain diffusional flow. *Acta Metallurgica* 26, 1379–1388.
- Balluffi, R., Allen, S., Carter, W., 2005. *Kinetics of Materials*. Wiley.
- Beere, W., 1976. Stress redistribution during Nabarro-Herring and superplastic creep. *Metal Science* 10, 133–139.
- Beere, W., 1977. Grain-boundary sliding controlled creep: its relevance to grain rolling and superplasticity. *Journal of Materials Science* 12, 2093–2098.
- Beere, W., 1978. Stresses and deformation at grain boundaries [and discussion]. *Philosophical Transactions of the Royal Society of London A: Mathematical, Physical and Engineering Sciences* 288, 177–196.
- Bilde-Sørensen, J., Smith, D., 1994. Comment on "Refutation of the relationship between denuded zones and diffusional creep". *Scripta Metallurgica et Materialia* 30, 383–386.
- Burton, B., 1994. Anisotropy of grain-boundary diffusional creep in a polycrystalline array with orthorhombic grain geometry. *Philosophical Magazine A* 69, 565–582.
- Burton, B., 2002. Diffusional rotation of crystals about a common interface. *Philosophical Magazine A* 82, 51–64.
- Cannon, W., 1972. The contribution of grain boundary sliding to axial strain during diffusion creep. *Philosophical Magazine A* 25, 1489–1497.
- Cannon, W., Langdon, T., 1988. Creep of ceramics. *Journal of Materials Science* 23, 1–20.
- Cannon, W., Sherby, O., 1977. Creep behavior and grain-boundary sliding in polycrystalline Al_2O_3 . *Journal of the American Ceramic Society* 60, 44–47.
- Chokshi, A., 2002. Diffusion creep in oxide ceramics. *Journal of the European Ceramic Society* 22, 2469–2478.
- Coble, R., 1963. A model for boundary diffusion controlled creep in polycrystalline materials. *Journal of Applied Physics* 34, 1679–1682.
- Cocks, A., 1994. The structure of constitutive laws for the sintering of fine grained materials. *Acta Metallurgica et Materialia* 42, 2191–2210.

- 686 Cocks, A., 1996. Variational principles, numerical schemes and bounding theorems for
687 deformation by Nabarro-Herring creep. *Journal of the Mechanics and Physics of Solids*
688 44, 1429–1452.
- 689 Cocks, A., Gill, S., Pan, J., 1998. Modelling microstructure evolution in engineering
690 materials. *Advances in Applied Mechanics* 36, 81–162.
- 691 Crossman, F., Ashby, M., 1975. The non-uniform flow of polycrystals by grain-boundary
692 sliding accommodated by power-law creep. *Acta Metallurgica* 23, 425–440.
- 693 Doghri, I., 2000. *Mechanics of deformable solids. Linear and nonlinear, analytical and*
694 *computational aspects.* Springer.
- 695 Duvaut, G., 1990. *Mécanique des milieux continus.* Dunod.
- 696 Fischer, F., Svoboda, J., Petryk, H., 2014. Thermodynamic extremal principles for irre-
697 versible processes in materials science. *Acta Materialia* 67, 1–20.
- 698 Fleck, N., Kuhn, L., McMeeking, R., 1992. Yielding of metal powder bonded by isolated
699 contacts. *Journal of the Mechanics and Physics of Solids* 40, 1139–1162.
- 700 Gibbs, G., 1966. Diffusion creep of a thin foil. *The Philosophical Magazine: A Journal of*
701 *Theoretical Experimental and Applied Physics* 13, 589–593.
- 702 Gibbs, G., 1968. The role of grain-boundary sliding in high-temperature creep. *Materials*
703 *Science and Engineering* 2, 269–272.
- 704 Gifkins, R., Langdon, T., 1970. Grain boundary displacements due to diffusional creep.
705 *Scripta Metallurgica* 4, 563–566.
- 706 Gleiter, H., Hornbogen, E., Baro, G., 1968. The mechanism of grain boundary glide. *Acta*
707 *Metallurgica* 16, 1053–1067.
- 708 Green, H., 1970. Diffusional flow in polycrystalline materials. *Journal of Applied Physics*
709 41, 3899–3902.
- 710 Greenwood, G., 1985. An analysis of the effect of multiaxial stresses and grain shape on
711 Nabarro-Herring creep. *Philosophical Magazine A* 51, 537–542.
- 712 Greenwood, G., 1992. A formulation for anisotropy in diffusional creep. *Proceedings of*
713 *the Royal Society of London A* 436, 187–196.
- 714 Hackl, K., Fischer, F., 2008. On the relation between the principle of maximum dissipation
715 and inelastic evolution given by dissipation potentials. *Proceedings of the Royal Society*
716 *of London A* 464, 117–132.
- 717 Herring, C., 1950. Diffusional viscosity of a polycrystalline solid. *Journal of Applied*
718 *Physics* 21, 437–445.
- 719 Herring, C., 1971. Reply to "The driving force for diffusion". *Scripta Metallurgica* 5,
720 273–277.
- 721 Hill, R., 1967. The essential structure of constitutive laws for metal composites and poly-
722 crystals. *Journal of the Mechanics and Physics of Solids* 15, 75–95.

- 723 Hötzer, J., Seiz, M., Kellner, M., Rheinheimer, W., Nestler, B., 2019. Phase-field simulation of solid state sintering. *Acta Materialia* 164, 184–195.
724
- 725 Huet, C., 1990. Application of variational concepts to size effects in elastic heterogeneous
726 bodies. *Journal of the Mechanics and Physics of Solids* 38, 813–841.
- 727 Keglinski, P., Wolf, D., Gleiter, H., 1998. Molecular-dynamics simulation of grain-
728 boundary diffusion creep. *Interface Science* 6, 205–212.
- 729 Kim, B.-N., Hiraga, K., Morita, K., Ahn, B.-W., 2004. Analysis of creep due to grain-
730 boundary diffusion in hexagonal microstructures. *Philosophical Magazine* 84, 3251–
731 3262.
- 732 Kim, B.-N., Hiraga, K., Morita, K., Chen, I.-W., 2005a. Rate of creep due to grain-
733 boundary diffusion in polycrystalline solids with grain-size distribution. *Philosophical*
734 *Magazine* 85, 2281–2292.
- 735 Kim, B.-N., Hiraga, K., Morita, K., Yoshida, H., 2005b. Effect of viscous grain-boundary
736 sliding on high-temperature deformation of nano-sized grains. *Review on Advanced*
737 *Materials Science* 10, 54–58.
- 738 Kim, B.-N., Hiraga, K., Morita, K., Yoshida, H., Ahn, B.-W., 2009. Viscous grain-
739 boundary sliding with rotating particles or grains. *Acta Materialia* 57, 5730–5738.
- 740 Kim, B.-N., Morita, K., Hiraga, K., 2003. Rate of diffusion creep accompanied by grain
741 boundary sliding in elongated microstructures. *Materials Science and Engineering A*
742 363, 67–71.
- 743 Lifshitz, I., 1963. On the theory of diffusion-viscous flow of polycrystalline bodies. *Soviet*
744 *Physics JETP* 17, 909–920.
- 745 McMeeking, R., Kuhn, L., 1992. A diffusional creep law for powder compacts. *Acta Met-*
746 *allurgica et Materialia* 40, 961–969.
- 747 Mishra, R., Jones, H., Greenwood, G., 1988. Enhanced diffusional creep: The effect of
748 grain growth. *Scripta Metallurgica* 22, 323–327.
- 749 Mori, T., Nakasone, Y., Taya, M., Wakashima, K., 1997. Steady-state creep rate of a
750 composite: Two-dimensional analysis. *Philosophical Magazine Letters* 75, 359–365.
- 751 Mori, T., Onaka, S., Wakashima, K., 1998a. Role of grain-boundary sliding in diffusional
752 creep of polycrystals. *Journal of Applied Physics* 83, 7547–7552.
- 753 Mori, T., Taya, M., Wakashima, K., 1998b. Steady-state creep of a composite analysed
754 by an energy balance method. *Philosophical Magazine Letters* 78, 331–338.
- 755 Nabarro, F., 1948. Report of a conference on the strength of solids. The Physical Society,
756 London 75.
- 757 Needleman, A., Rice, J., 1980. Plastic creep flow effects in the diffusive cavitation of grain
758 boundaries. *Acta Metallurgica* 28, 1315–1332.

- 759 Onaka, S., Huang, J., Wakashima, K., 1998. Kinetics of stress relaxation caused by the
760 combination of interfacial sliding and diffusion: two-dimensional analysis. *Acta Mate-*
761 *rialia* 46, 3821–3828.
- 762 Onaka, S., Madgwick, A., Mori, T., 2001. Kinetics of diffusional creep discussed by energy
763 dissipation and effect of grain-size distribution on the rate equations. *Acta Materialia*
764 49, 2161–2168.
- 765 Pan, J., Cocks, A., 1993. Computer simulation of superplastic deformation. *Computa-*
766 *tional Materials Science* 1, 95–109.
- 767 Rachinger, W., 1952-1953. Relative grain translations in the plastic flow of aluminium. *J.*
768 *Inst. Metals* 81, 33.
- 769 Raj, R., Ashby, M., 1971. On grain boundary sliding and diffusional creep. *Metallurgical*
770 *Transactions* 2, 1113–1127.
- 771 Ruano, O., Wadsworth, J., Sherby, O., 2003. Deformation of fine-grained alumina by
772 grain boundary sliding accommodated by slip. *Acta Materialia* 51, 3617–3634.
- 773 Spingarn, J., Nix, W., 1978. Diffusional creep and diffusionally accommodated grain re-
774 arrangement. *Acta Metallurgica* 26, 1389–1398.
- 775 Suo, Z., 1997. Motions of microscopic surfaces in materials. *Advances in Applied Mechan-*
776 *ics* 33, 193–294.
- 777 Wang, J., 2000. Investigation of the deformation mechanism in grain size-sensitive New-
778 tonian creep. *Acta Materialia* 48, 1517–1531.
- 779 Wang, Y.-J., Ishii, A., Ogata, S., 2011. Transition of creep mechanism in nanocrystalline
780 metals. *Physical Review B* 84, 224102.
- 781 Wei, Y., Bower, A., Gao, H., 2008. Recoverable creep deformation and transient local
782 stress concentration due to heterogeneous grain-boundary diffusion and sliding in poly-
783 crystalline solids. *Journal of the Mechanics and Physics of Solids* 56, 1460–1483.